

Morphology, microstructure and magnetic properties of thermionic vacuum arc deposited NiFeCu ferromagnetic thin films

Viorel IONESCU^{a*}, Gabriel PRODAN^a, Ionut JEPUB^b, Ion MUSTATA^b,
Cristian Petrica LUNGU^b and Eugeniu VASILE^c

^aUniversity of Constanta, Physics and Electronics Department, 124 Mamaia Blvd, 900527 Constanta, Romania

^bNational Institute for Lasers, Plasma and Radiation Physics, Magurele-Bucharest, 077125 Romania

^cMetav-CD S.A., Bucharest, 050025, Romania

Abstract NiFeCo granular ferromagnetic thin films were deposited on glass and silicon wafer substrates in thermionic vacuum arc plasma with simultaneous ignition of plasma in Cu and NiFe vapors. The structural and morphological properties of the prepared films were investigated by TEM Transmission Electron Microscopy (TEM) and Scanning Electron Microscopy (SEM). Elemental composition of the films was revealed after X-ray energy dispersive spectroscopy analysis (EDAX). The magneto-optical longitudinal Kerr rotation spectra of the samples were also measured and compared.

Keywords: TVA method, HRTEM, MOKE measurements

1. Introduction

The granular ferromagnetic thin films are composite materials that consist usually in nanometric magnetic grains (Fe, Co) uniformly distributed within a nonmagnetic matrices (copper, silver or gold). Granular systems like CoAg, FeCu, CoCu and FeCoCu are able to produce both positive and negative electrical resistance variation under the influence of an external magnetic field, effect named Giant Magnetoresistive Effect (GMR) [1-5]. This effect is due to the spin-dependent scattering taking place at the boundaries of ferromagnetic clusters embedded in the nonmagnetic host lattice. The other magnetic properties, such magneto-optical Kerr effect (MOKE) have been found in those granular magnetic solids [6- 8].

Because of their enhanced magnetic properties and magneto-transport characteristics, these structures are called soft ferromagnetic materials having important applications in the microelectronic devices like linear and circular position sensors [9, 10], reading hard drives heads, and microwave devices.

Because of the immiscibility of some transition metals with noble metals, in the case of granular systems it is possible to obtain a mixture of a nonmagnetic matrix with precipitated magnetic

entities. It is also possible to obtain the granular structure straight away by sputtering deposition from the composite material target [11].

The concentrations of elements are chosen in such a way that an application of a heat treatment enables the coalescence of the magnetic material, originating magnetic clusters [12].

The properties of these magnetic clusters (e.g., average size, size distribution, concentration) determine the magnetic behavior of the granular film, and its characterization is of key importance to understand the GMR phenomena [13].

One of the most proper base materials used for GMR sensors is the granular NiCuFe layer which combines the Anisotropic Magnetoresistance (AMR), low signal with high electric conductivity and low coercivity. It was used copper to suppress the magnetoresistive signal below of the NiFe, and the optimal concentration of the thin film structures included 30%-65% Ni, 5%-25% Fe and 10%-40% Cu[14]. For this type of granular films Ni atoms can make solid connection with the Cu atoms, generating possible granular alloys of Cu-Ni and Fe-Ni, respectively [15].

In this study we proposed to investigate the substrate type influence upon the microstructural, morphological and Kerr magneto-optical properties of a series of NiFeCu granular thin film samples

deposited by termionic vacuum arc (TVA) technique; this method proved to be very successful for the deposition of nanostructured granular films, unstressed, continuous and smooth [17], the metal-insulator granular films showing the presence of magneto-optical Kerr effect [18].

2. Experimental

This method allows, as can be seen in **Fig. 1**, the simultaneous deposition of granular films with different NiFe - Cu concentrations and different size of the magnetic clusters, giving rise to the possibility of a detailed examination of microstructural and morphological correlations concerning MOKE phenomena.

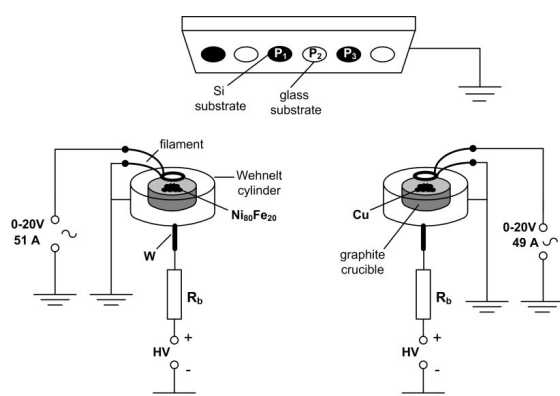


Fig.1. The experimental set-up for the NiFeCu thin film deposition.

The anodes were a graphite crucible filled with a high purity NiFe alloy formed by 80 at. % Ni and 20 at. % Fe and another crucible filled with 99, 99% purity metal flakes of Cu. The deposition substrates were BK7 optical glass and silicon (111) disks.

The emitted electrons beams provided by the TVA guns are accelerated by high anodic voltages (1-6kV), being focused by two Wehnelt cylinders.

The tungsten filament of the NiFe cathode was heated by an a.c. current of 51A, and the heating current of the Cu cathode was 49A.

The applied d.c. voltage for the bright discharge in NiFe vapors was 590-630 V, the intensity of arc current being 1.3-1.5 A. In the case of the discharge ignited in Sn vapours, the d.c. voltage was about 700-740V and the d.c. current intensity between 0.5-

0.6A. The pressure inside the deposition chamber was maintained at a value of about 6.6×10^{-6} Torr.

The deposition rate r_d and film thickness d were measured and controlled *in situ* using a FTM7 quartz microbalance. The thickness of the obtained samples was of about 200 nm.

The samples investigated, named P_1 , P_2 and P_3 , were deposited on silicon substrate (P_1 and P_3) and a glass substrate (P_2). The samples, ordered in a decreasing NiFe relative content, were positioned at the following distances from the NiFe/Cu anodes, respectively: 28 cm/34 cm – P_1 , 30 cm/32 cm – P_2 and 32 cm/30 cm – P_3 .

Transmission Electron Microscopy (TEM) analysis were carried out by a Philips CM120ST microscope operating at 100 kV with $C_s = 1,2\text{mm}$ and $\approx 2 \text{ \AA}$ resolution.

The SEM measurements were carried out using a FEI- Philips Quanta Inspect F streak scanning electron microscope equipped with secondary electron detector (ETD), with 1.2nm resolution in a 30kV secondary electron image.

The compositional analysis of the film was accomplished using an energy dispersive x-ray spectroscopy (EDAX) microanalysis detector attached to the SEM, with resolution of 132 eV at Mn K α .

The magneto-optical Kerr effect (MOKE) is a powerful tool for studying changes in the surface magnetization of granular ferromagnetic films, at depths in the film up to 20nm.

The magnetic properties of the NiFeCu films were investigated via longitudinal Magneto-Optic Kerr Effect (MOKE), using p-polarized, 633 nm He-Ne laser light (10 mW power) as an incident light. The incident beam was modulated with an electro-optic-modulator. The magnetic field was applied parallel to the films and lays in the incidence plane of He-Ne laser.

3. Results and Discussions

From bright field (BF) - TEM images presented in **Fig. 2** we can see the presence of some nanometrical conglomerates (dark areas), which could be associated with ferromagnetic elements Fe and Ni, fixed in a lighter nonmagnetic matrix of Cu.

The size distributions of the crystallites, obtained from the diameter measurements of a few

dozen grains highlighted in fig. 2 are plotted in **Fig.3**.

The distribution of grain sizes, as measured from TEM images, was fitted to the lognormal curve. The mean grain size, D_m , was found to be approximately 7 nm in the case of the sample P₁ and 5 nm for sample P₂.

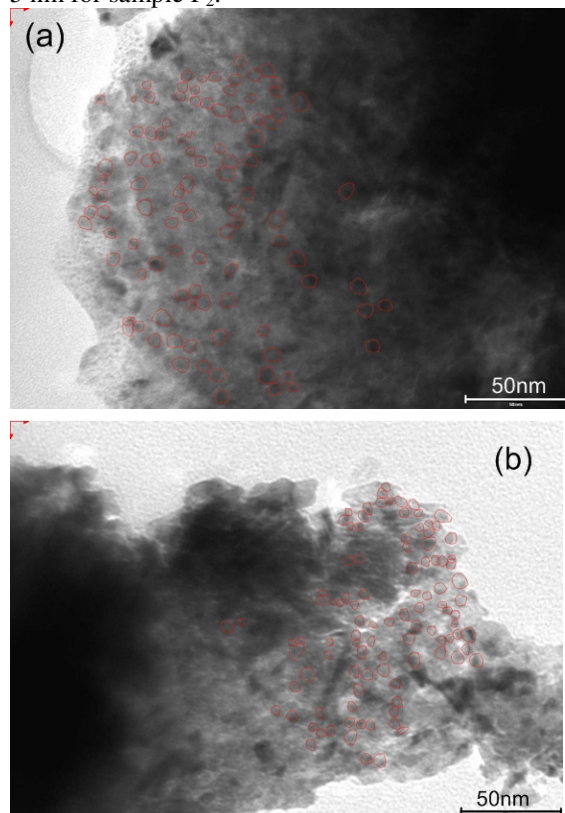


Fig.2. BF-TEM images of : a) P₁ sample, on silicon substrate; b) P₂ sample, on glass substrate.

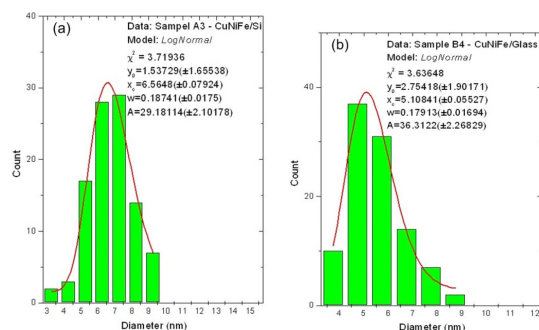


Fig.3. Grain size distribution of NiFeCu granular film: (a) P₁ sample, (b) P₂ sample.

High resolution transmission electron microscopy (HRTEM) images of NiFeCu samples are shown in **Fig. 4**. Electron diffraction patterns evidence a nice structure with well-arranged atomic planes located on different areas (darker and lighter) of the sample, with different inter-planar distance (see fig.4.b), suggesting the presence of minimum two different crystalline species in the probes investigated.

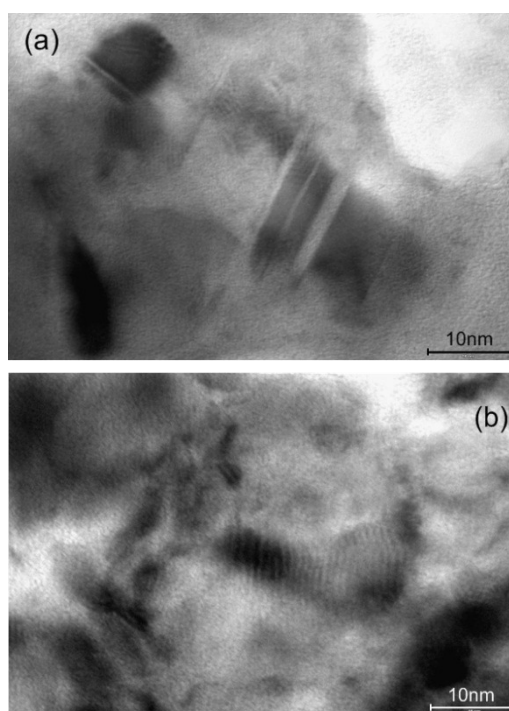


Fig.4. HRTEM images of: a) P₁ sample and b) P₂ sample.

The well-defined diffraction rings from selected area electron diffraction (SAED) patterns (see **Fig. 5**) indicate also the polycrystalline state of the thin film investigated. Almost all interplanar distances corresponding to diffraction rings shown in those patterns fits well with the diffraction planes distances for the fcc phase of Cu, just the first ring being associated with fcc crystalline phase of Fe; because Ni and Cu have a very similar crystallographic structure and those metals can form a solid solution, no nickel diffraction rings could be established in SAED patterns.

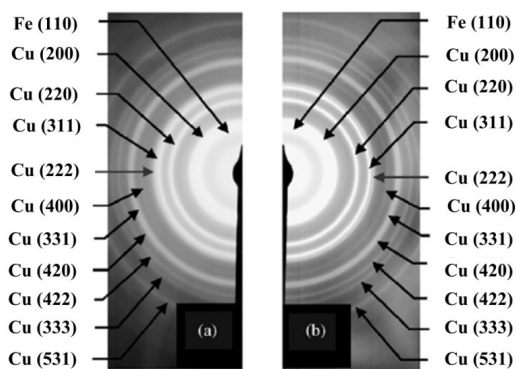


Fig.4. SAED patterns of NiFeCu thin film samples: a) P₁ and b) P₂

Cross-sectional SEM analysis was used to establish the quality of the deposition and the thickness of the thin film. The sample was examined in cross section by cutting with glasses cutter(diamond) the uncovered surface, and after that the sample was put in the liquid nitrogen, fracture being in this way produced .

In the SEM images at 50.000 x magnitude showed in **Fig. 5.a** and **6.a**, details are observed in the cross – section of the thin film deposition on the substrate (with horizontally band light on the image); both samples presented an compact, crack-free surface morphology close to film fracture. The measured thickness was 158.3 nm for P₁ sample and 157.5 nm for P₂ sample.

The morphological surface SEM images from **Fig. 5.b** and **6.b**. showed a fairly compact, dense and smooth surface of NiFeCu films, with uniform distribution of grain size(under 100nm) over total coverage of the substrates.

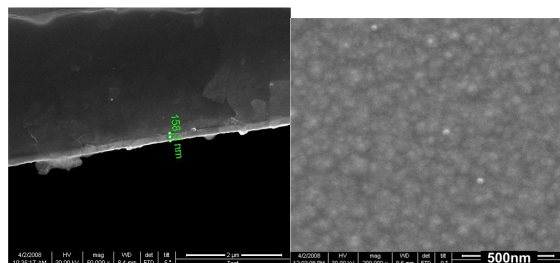


Fig. 5.a) Cross-sectional and b) morphological surface secondary electron SEM images of P₁ sample

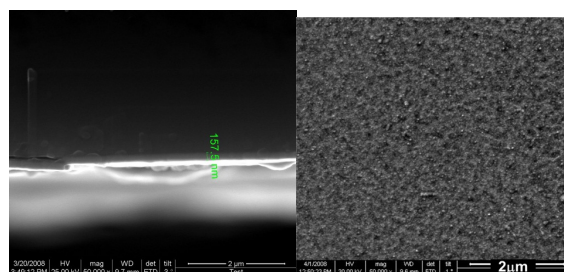


Fig. 6. a) Cross-sectional and b) morphological surface secondary electron SEM images of P₂ sample

The X-ray energy dispersive spectroscopy analysis of P₁ sample (**Fig. 7**) revealed the presence of the main elements Cu, Ni and Fe, in the cross-section of the film. The Si element in the EDAX spectrum comes from the substrate on which the deposition was made, the contamination species C and Mn being provided by anode crucible. From the maps with density concentration distribution of each element (see also fig.7), we could observe a very compact density distribution for the sample constituent metals, especially for Cu.

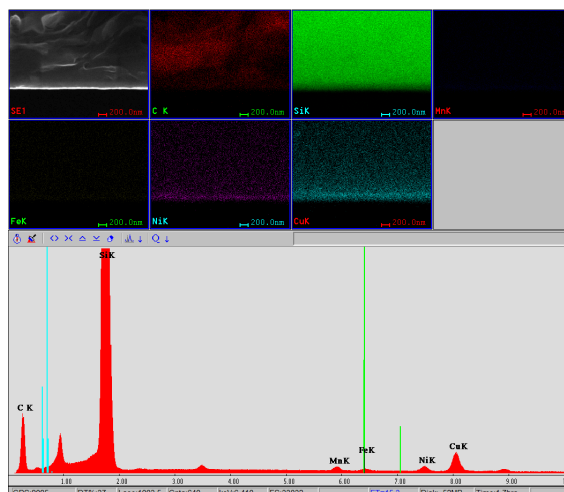


Fig.7. EDAX spectrum and maps with density concentration distribution for the constituent species of P₁ sample

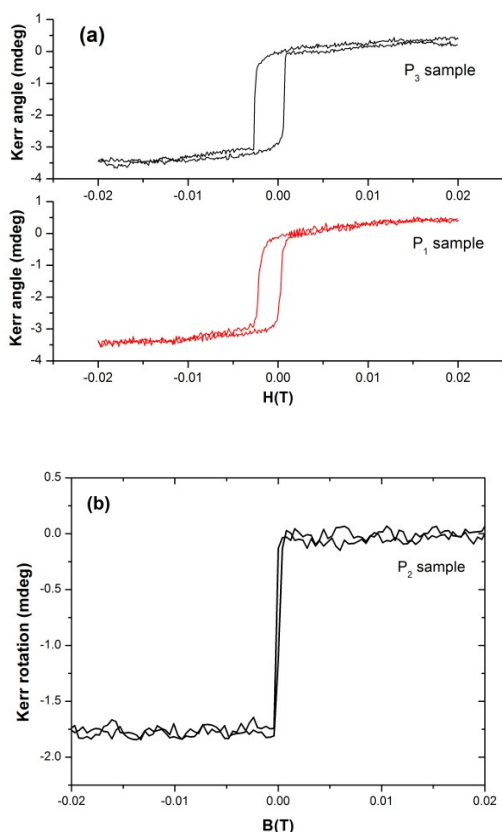


Fig.8. MOKE measurements on samples P_1 , P_3 (a) and P_2 (b) at room temperature.

In **Fig. 8** we present the MOKE hysteresis loops (longitudinal mode) at room temperature for samples P_1 , P_2 and P_3 . It can be observed that the saturation magnetization for sample P_1 and P_3 (of about 1.5 mdeg) is about two times higher than that of the P_2 sample; the coercivities resulting from MOKE measurements are 1.75mT and 1.9mT for P_1 and P_3 sample, respectively; in the case of P_2 sample, it was observed a very small coercivity of 0.1mT, this probe entering first in saturation and containing the ferromagnetic (NiFe) particles with the largest diameter.

4. Conclusions

The granular ferromagnetic NiFeCu films with thickness of 157-158 nm were successfully

deposited onto glass and silicon substrates using the TVA method.

Microstructural BF-TEM investigations showed the nanocrystalline state of the films, cross-section investigations revealing the presence of some conglomerates with 5 nm and 7nm in diameter, for sample on glass and silicon substrate, respectively.

HRTEM and SAED analysis indicated the existence of different crystalline species in the samples, the cubic crystallographic structure of Cu and Fe being established this way.

The morphological SEM images suggested that both samples investigated had a compact and fine grained morphology at the surface, with grain diameters under 100 nm. EDAX spectrum indicated the presence of main elements: Cu, Ni, Fe in the film, with a compact density distribution.

Sample deposited on glass substrate presented after MOKE measurements the lowest coercivity, but the saturation magnetization was two times smaller than in the case of the sample on silicon substrate, this property indicating lower magnetic properties of the sample on glass substrate.

5. References

- * E-mail address: ionescu.vio@gmail.com
- [1] H. Sang, G. Ni, J.H. Du, N. Xu, S.Y. Zhang, Q. Li and Y.W. Du, *Appl.Phys. A* **63** 167-170 (1996).
 - [2] J.Q.Xiao, J.S.Jiang and C.L.Chien, *Phys. Rev. Lett.* **68**, 3749-3752 (1992).
 - [3] A. E. Berkowitz, J. R. Mitchell, M. J. Carey, A. P. Young, S. Zhang, F. E. Spada, F. T. Parker, A. Hutten, and G. Thomas, *Phys. Rev. Lett.* **68**, 3745 - 3748 (1992).
 - [4] J. Vergara and V. Madurga, *J. Non-Crystalline Sol.* **287**, 385-389 (2001)
 - [5] S.H. Ge, Y.Y. Lü, Z.Z. Zhang, C.X. Li, T. Xu and J.Z. Zhao, *Journal of Magnetism and Magnetic Materials* **168**, 35-42 (1997).
 - [6] W. Yang, Z. S. Jiang, J. H. Cai, Y. W. Du, S. M. Zhou, L. Y. Chen and R. J. Zhang, *Journal of Magnetism and Magnetic Materials* **177**, 1289-1290(1998).
 - [7] W. M. Zheng, L.Y. Chen and J.H. Chu, *Physica Status Solidi B* **214**, 463-469 (1999).
 - [8] P. Vavassori, E. Angeli, D. Bisero, F. Spizzo and F. Ronconi, *Appl. Phys. Lett.* **79** (14), 2225 - 2227 (2001).

- [9] S. Arana, E. Castano and F.J. Gracia, IEEE Sens. J. **4**, 221-225 (2004).
- [10] S. Arana, N. Arana, R. Gracia and E. Castano, Sens. Actuat. A: Phys. **123**, 116-121 (2005).
- [11] J.Q. Wang and G. Xiao, Phys. Rev. B **49**, 3982–3986 (1994).
- [12] P. Allia, P. Tiberto, M. Baricco and F. Vinai, Rev. Sci. Instrum. **64**, 1053 (1993).
- [13] A.E. Berkowitz, J.R. Mitchell, M.J. Carey, A.P. Young, D. Rao, A. Starr, S. Zhang, F.E. Spada, F.T. Parker, A. Hutten and G. Thomas, J. Appl. Phys. **73** 5320 (1993).
- [14] D. Macken, M.K. Minor, S.B. Slade, D.J. Larson and D.J. Dummer, United States Patent No.7, 139,165 B2, Oct.31, 2006.
- [15] H. Fujimori, S. Mitani and S. Ohnuma, Mater. Sci. Eng. B **31**, 219–223 (1995).
- [16] C.P. Lungu, I. Mustata, G. Musa, A.M. Lungu, O. Brinza, C. Moldovan, C. Rotaru, R. Iosub, F. Sava, M. Popescu, R. Vladoiu, V. Ciupina, G. Prodan and N. Apetroaei, J. Optoelectron. Adv. Mater. **8**, 74 (2006).
- [17] V. Kuncser, I. Mustata, C.P. Lungu, A.M. Lungu, V. Zaroschi, W. Keune, B. Sahoo, F. Stromberg, M. Walterfang, L. Ion and G. Filoti, Surface & Coatings Technology **200**, 980 – 983 (2005).
- [18] V. Ionescu, M. Osiac, C.P. Lungu, O.G. Pompilian, I. Jepu, I. Mustata and G.E. Iacobescu, Thin Solid Films **518**, 3945–3948 (2010).
- [19] C. P. Lungu, I. Mustata, A. M. Lungu, O. Brinza, V. Zaroschi, V. Kuncser, G. Filoti and L. Ion, J. Optoelectron. Adv. Mater. **7**(5), 2507-2512 (2005).

Submitted: January 22th 2012

Accepted in revised form: March 30th 2012